Correlation of Regional Disease and In Vivo P_{O_2} *in Rat Mammary Adenocarcinoma*

MARK A. COLE, MS,
DONALD W. CRAWFORD, MD,
NANCY E. WARNER, MD,
and HAROLD W. PUFFER, PhD

From the Departments of Pathology and Medicine, Cardiology Division, University of Southern California School of Medicine, Los Angeles, California

A knowledge of the distribution of oxygen tension (P_{O_2}) and vascularization in neoplasia has been fundamental to understanding relationships between tumor growth, hypoxia, and therapy. We have combined recessed oxygen microcathode and freeze-substitution techniques to correlate *in situ* P_{O_2} profiles and morphologic features in 7,12-dimethylbenz(a)anthracene (DMBA) tumors in rats. Overlying connective tissue of transplanted tumor was exposed by a 1–2 mm incision and a cross-stitch pattern demarcated electrode puncture sites for histologic reference. Three buffered salt solutions (BSS) with different P_{O_2} were each allowed to flow through a well over the tumor where electrodes were placed for calibration. Zero electrode oxygen current was recorded from a buffered yeast–agar mixture of zero torr. P_{O_2} was recorded at 5-μ intervals to approximately 1–2 mm. Atmospheric contamination was eliminated by continuous well flow of BSS, 30 torr. Finally, the tumor and surrounding tissues were quick-frozen *in vivo* with Freon 22 and liquid nitrogen. The tissue block was freeze-substituted and sectioned. P_{O_2} profiles were superimposed onto correspondingly scaled photomicrographs. A viable periphery with a P_{O_2} range of 50–82 torr and a transition to necrotic areas of P_{O_2}, 2–13 torr were observed. This transition was characterized by P_{O_2} gradients within distances of 50–300 μ at variable puncture depths. This technique should be useful in further studies of growth, necrosis, and therapy. (Am J Pathol 1983, 112:61–67)

FUNDAMENTAL to understanding the relationship between tumor growth, hypoxia, cellular metabolism, and radiosensitivity has been a knowledge of the oxygen distribution within the neoplasm. The exploration of *in vivo* oxygen distribution in neoplasia was pioneered by Cater and Silver[1,2] and studied by others.[3–6] However, oxygen studies in tumors thus far have been difficult to interpret or evaluate, primarily because of the problems with experimental techniques. For example, it is questionable whether oxygen microcathodes used in previous studies can be accurately calibrated for tissue measurements.[7] Platinum wire oxygen electrodes have been used to measure tissue P_{O_2}, but these large electrodes might compress and damage tissue.[8,9] Atmospheric contamination created an oxygen diffusion gradient extending into the tissue, influencing electrode measurements.[10] Membrane-coated needles or bare-tipped electrodes have reduced but have not necessarily eliminated an induced P_{O_2} field surrounding the electrode.[7] Consequently, electrode current response was not accurately converted to tissue P_{O_2} even in the center of the tumor, where atmospheric contamination was not a significant factor. Finally, oxygen distribution has not been correlated with morphologic characteristics.

To correlate regional morphology of rat adenocarcinoma (AD) with concentration of oxygen in tissue *in vivo*, we measured intracellular P_{O_2} profiles in transplanted 7,12-dimethylbenz(a)anthracene (DMBA) mammary adenocarcinoma using a recessed microcathode (diameter $\leqslant 4\mu$). We conducted the experiments inside a Faraday cage to eliminate electrical interference.[11] The oxygen electrode was recessed and was so constructed that surrounding oxygen diffusional fields were limited to

Supported in part by an NHLBI Program Project Grant HL23619 and an American Cancer Society Institutional Research Grant IN-21-U to the LAC-USC Comprehensive Cancer Center.

Accepted for publication March 4, 1983.

Address reprint requests to Mark A. Cole, USC School of Medicine, 2025 Zonal Avenue HMR 810, Los Angeles, CA 90033.

0002-9440/83/0707-0061$01.15

about 2 μ, thus permitting calibration in a liquid medium for measurement of P_{O_2} in tissues.[11,12] Representative *in situ* dimensions were preserved on permanently stained histologic sections by a freeze-exchange process.[11,13] The results of these studies are described in this article.

Materials and Methods

Electrode Construction and Calibration

Electrodes were constructed according to Whalen[12] and Crawford.[11] Briefly, glass capillary pipettes were filled with Wood's metal (which ultimately serves as the primary conductor) and pulled to microscopic points with a Kopf pipette puller. With a rotating drum covered with synthetic diamond dust, the point was beveled to 30–50 degrees with the base of the bevel expanding to approximately 4 μ. A recess of 15–20 μ was formed within the glass lumen (usually 1.0–1.5 μ in diameter). By electroetching, the Wood's metal was removed from the distal 15–20 μ of the pipette, forming a recessed tip. By electroplating, a 4–5-μ column of gold was applied to the end of the column of Wood's alloy in the tip of the pipette. Final recess length–lumen diameter ratios were greater than 7.5. The gold column within the recess in the tip served as the site for actual electrochemical reduction of diffused oxygen. With vacuum release, the remaining recess was filled with a hydroxymethacrylate hydrogel plug, which forms a geometric lattice after polymerization (Figure 1). This lattice enables oxygen to diffuse to the gold surface while excluding large molecular weight compounds such as protein (which might form sulfhydryl combinations with the gold surface, resulting in unstable electrode response). We calibrated the electrodes in an insulated 5-ml beaker using three buffered salt solutions (BSS) bubbled, respectively, with gas mixtures of 21%, 12.5%, and 1.5% oxygen, 4–5% carbon dioxide, and balanced with nitrogen at approximately 40 C. BSS was sampled during microcathode current recordings, and oxygen levels in the BSS were measured with a Radiometer PSM-71 (Radiometer Co., Copenhagen, Denmark) and averaged 140, 90, and 25 torr, respectively. The resulting pH of each BSS ranged from 7.43 to 7.47. Since our tumor model characteristically developed necrotic regions, we extended our low calibration range to 0 P_{O_2} torr, using a yeast-agar ($K_m \simeq 0.3$ mm Hg oxygen) mixture at a pH of approximately 7.4.[14] Therefore, four calibration measurements ranging from 0 to approximately 145 torr oxygen were recorded, and the ampere versus P_{O_2} response (Figure 2) was always linear ($r^2 > 0.99$). Standard deviation from the regression varied from 0 to 3 torr. The recessed electrode limited the diffusion of oxygen from the surrounding environment and permitted calibration in a liquid medium for measurement of P_{O_2} in tissues.

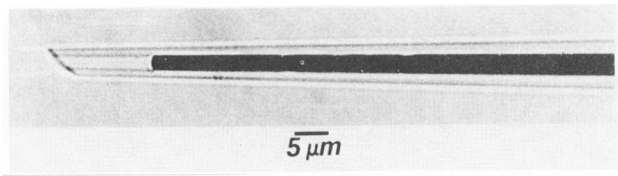

Figure 1 – Photomicrograph of a recessed oxygen microcathode. The recess has been filled with a hydroxymethacrylate polymer and hydrated. Diameter at the tip of the bevel is approximately 4 μ.

Animal Preparation and Experimental Protocol

Fischer 344 female rats were lightly anesthetized by methoxyflurane inhalation. Fragments of DMBA-induced rat mammary adenocarcinoma of approximately 1 cu mm were transplanted into the right inguinal area by trocar. After 1½–3 weeks, when the tumors had grown to 2–12 mm in diameter, rats were again anesthetized with an intraperitoneal injection of 50% urethane–50% chlorolose mixture. The connective tissue overlying the tumor was exposed by a 2-mm cutaneous incision. If surgical trauma produced hemorrhage, the animal was discarded. A soft plastic cuff was then sewn to the skin surrounding the

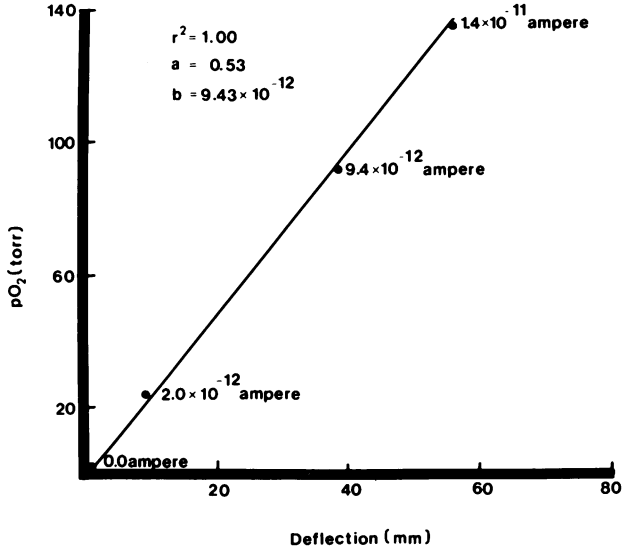

Figure 2 – Sample calibration of a recessed oxygen microcathode. The ordinate is P_{O_2} (mm Hg), and the abscissa is deflection (mm). Ampere values correspond to deflection points. The standard regression line is shown. *a* is the intercept; *b* is the slope; r^2 is the regression coefficient.

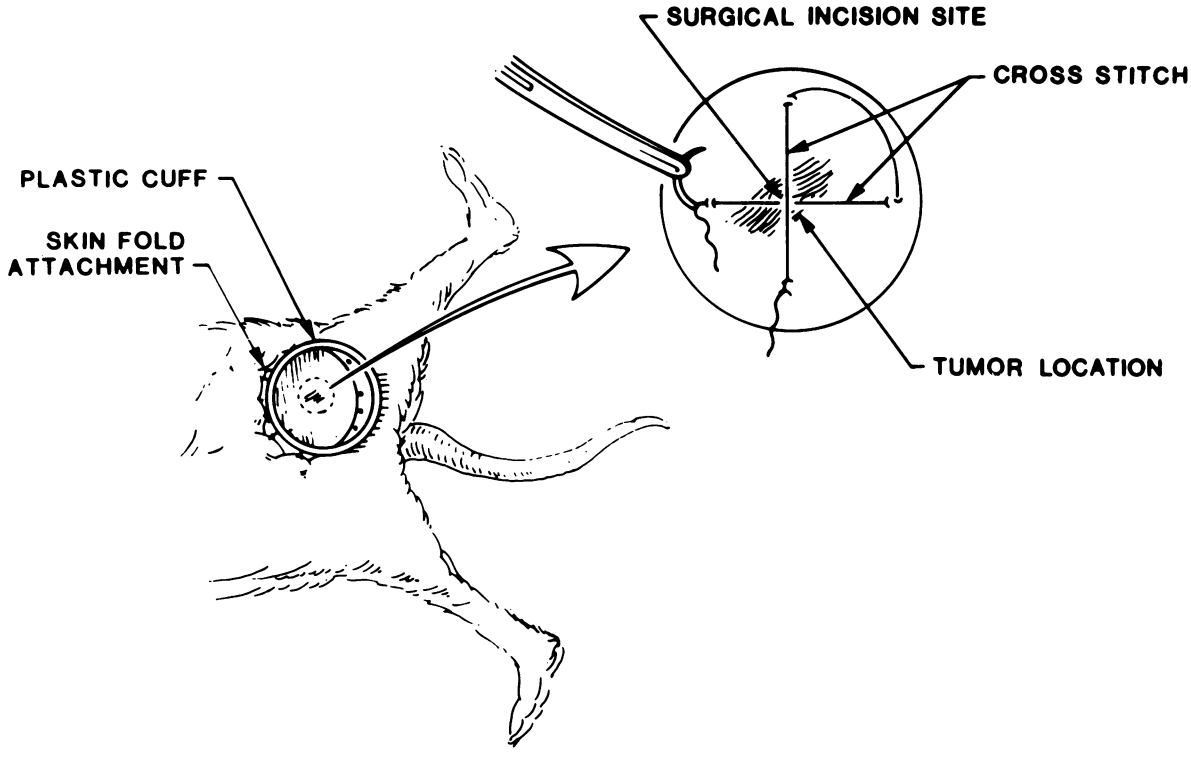

Figure 3—Illustration of animal preparation. Overlying connective tissue is surgically exposed, and a cross-stitch is sewn to the skin folds (*upper right*).

tumor to form a well, and a cross-stitch suture pattern was sewn to incision skin folds (Figure 3). The plastic well localized the buffers during the experiment and facilitated *in situ*, *in vivo* quick freezing of the tumor and surrounding tissue. The cross-stitch formed a landmark that divided the exposed surface of the tumor into quadrants, and nearly all puncture sites were situated within 0.5 mm from the suture.

All experiments were done inside a Faraday cage from which all detectable alternating current had been excluded. The animal's position was fixed on a modified Kopf stereotactic base placed on a pneumatically mounted table that dampened detectable vibrations. The base plate supported a mechanical three-directional micromanipulator. A Kopf stepping hydraulic microdrive slave cylinder capable of 1-μ discrimination was attached to the micromanipulator. We advanced the electrode at preset intervals of 5, 10, and 20 μ. To avoid compression of the tissue during puncture, a calibrated miniature speaker cone was attached to the microdrive slave cylinder.[15] One end of a machined Lucite rod was attached to the armature of the speaker-cone and the other end held a female connector pin into which the electrode connector was inserted. The loudspeaker was driven between 200 and 500 Hz during puncture, with the amplifier gain set to minimize vertical motion in tissue to 2–4 μ. We did not observe any compression under the dissecting microscope, nor did an altered electrical signal suggest tissue indentation.

For calibration during the experiment, the three BSSs and the yeast-agar mixture of known P_{O_2}'s of approximately 140, 90, 25, and 0 torr were again recorded. Using the dissecting microscope, the solution in the well was completely aspirated, and the electrode was advanced in micron increments until tissue contact was confirmed by an oxygen current signal. Atmospheric contamination of the site was eliminated by then filling the well with continuously flowing BSS of 30-torr P_{O_2}, which approximated the oxygen concentration of subcutaneous tissue. This P_{O_2} level was important because oxygen gradients extending from BSS (of approximately 90 torr) into tissue surface regions have been previously measured and have influenced tissue oxygen levels.[11] The electrode was advanced to a depth of 0.8 to 2.0 mm, usually at 5-μ increments, and oxygen current recordings were made. These recordings are termed an "oxygen profile." Occasionally, when large differences in the current of the microcathode were observed, electrode advancement was momentarily delayed until a plateau current was recorded. The electrode was with-

drawn, and recordings were made usually at 10-μ increments to the surface of the tissue. Recalibration was then done in the superfusion solution.

In vivo morphologic characteristics were preserved by the following freeze-substitution fixation method derived from the original methods of Giese and others.[13,16-18] At the conclusion of the experiment, Freon 22 at −21 C was cooled to approximately −160 C in liquid nitrogen. Without disturbing the animal's position, cooled Freon was poured over the incision contained in the well formed by the plastic cuff. The liquid Freon froze a solid block of tumor and surrounding tissue. Seconds afterwards, the animal was sacrificed by an intravenous injection of sodium pentobarbital. Next, liquid nitrogen at −196 C was poured on the site. After a thorough freeze was evident, the tumor and surrounding tissue were excised with a cast cutter. The frozen block was then placed for 2 weeks in acetone at −70 C followed by absolute alcohol at −70 C. Acetone, which had no significant effects on tissue volume at −70 C, served as a good primary fixative.[18] The tissue was then placed in 50% ether–50% alcohol for 24 hours at room temperature and then for 2 weeks each in 10%, 25%, and 50% celloidin in ether–alcohol. The block was desiccated, mounted, and cut at an average of 50 μ. Hemotoxylin and picrofuchsin were used for staining.

Correlation of Oxygen Profile With Morphologic Features

Raw data from each puncture was entered into a laboratory instrumentation computer (Digital Equipment, Culver City, Calif, PDP 11/03). The calibration regressions were calculated, and conversion from electrode current response to the P_{O_2} of each traverse was accomplished and then graphed (P_{O_2} versus depth of puncture). Photomicrographs were taken of serial sections in the area of the cross-stitch over the tumor at the approximate puncture site location. Overlays of the P_{O_2} profiles were superimposed onto the correspondingly scaled photomicrographs.

Results

In general, viable regions of the tumor had a P_{O_2} level of 50–70 torr; whereas the necrotic zones had levels of 2–12 torr. Figure 4 shows a representative example of a freeze-substituted section of adenocarcinoma with a superimposed P_{O_2} profile. The periphery of the tumor (P) was well vascularized, with a network of small and medium sized vessels (V). Next was a region of areas of "hit-or-miss necrosis" (N). The interior of the tumor (I) was necrotic and liquefied. The P_{O_2} profile of this adenocarcinoma was superimposed so that the region of the point of the

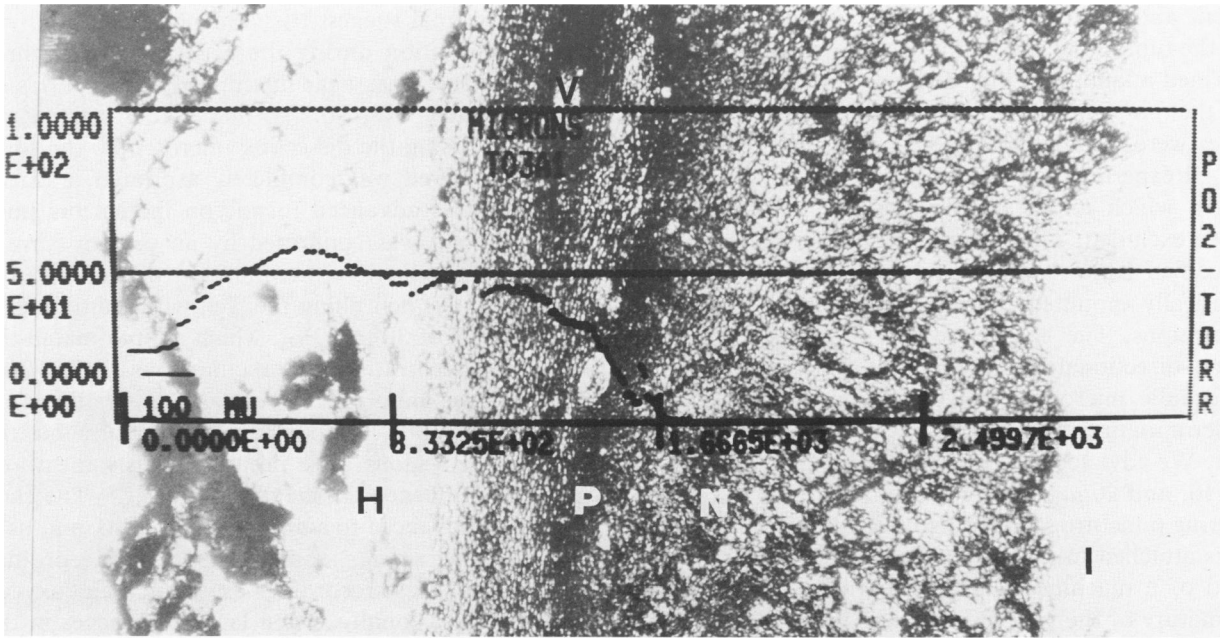

Figure 4 — A freeze-substituted section of an adenocarcinoma with a superimposed P_{O_2} profile (Tumor 3). The abscissa is the depth of puncture in microns, and the ordinate is P_{O_2} torr (note that decimal places cannot be suppressed in the computer operating system). *P*, periphery of tumor; *V*, vessels; *N*, "hit-or-miss" necrosis; *I*, the interior of the tumor; *H*, hypodermis. (×42)

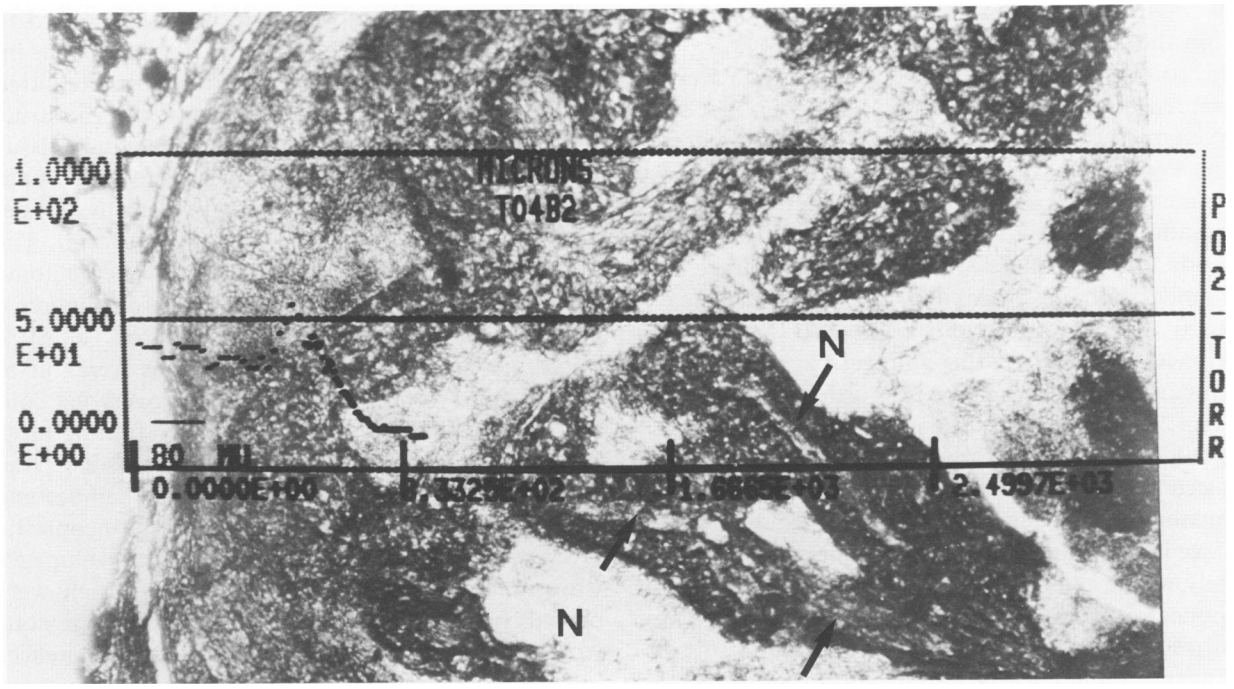

Figure 5—A freeze-substituted section of an adenocarcinoma with a superimposed P_{O_2} profile (Tumor 4). The abscissa is the depth of puncture in microns, and the ordinate is P_{O_2} torr (note that the decimal places cannot be suppressed in the computer operating system). The *arrows* indicate longitudinally cut vessels. *N*, central necrotic regions. (×42)

electrode contact is 0 μ on the abscissa and corresponds to the region of contact of the electrode, as marked by the location of the suture. This particular tumor displayed a 40–45 torr P_{O_2} gradient from viable periphery to necrotic regions over a range of 100–125 μ.

Figure 5 is another P_{O_2} profile of a different tumor and shows similar morphologic features with interesting longitudinally cut vasculature networks (arrows) surrounded by central geographic necrotic regions (N) with viable AD cells forming a mantle around vascular channels. This tumor showed a 30–40 torr P_{O_2} gradient from viable tumor cells to necrotic regions over a range of approximately 150 μ.

Table 1 summarizes the data obtained from 4 separate tumors and 7 different P_{O_2} profiles. Viable tumor P_{O_2} ranged from 50 to 70 torr. Necrotic tumor P_{O_2} ranged from 2 to 13 torr. We found that each tumor displayed this P_{O_2} range and noted a range of transition of 50–300 μ from viable to necrotic tissue.

Discussion

This study has presented a technique for correlating tumor oxygen distribution with morphologic features. Table 1 summarizes the P_{O_2} data obtained from 4 separate tumors. P_{O_2} levels of 50–82 torr were associated with viable tissue, in contrast to necrotic regions, where P_{O_2} was observed to range from 2 to 13 torr.

Previously reported values might be low estimates of actual tissue P_{O_2} because of the type of electrode used.[7] Small needle-type and bare-tipped electrodes which are membrane-coated have reduced, but have not necessarily eliminated, an induced P_{O_2} field. Consequently, these electrodes have not accurately converted current to tissue P_{O_2}; hence, oxygen levels were not measured accurately in the center of the tumor or in surface regions where atmospheric oxygen contamination was an important factor. Atmospheric contamination created an oxygen diffusion gradient that extended into the exposed tissue,

Table 1—Summary of P_{O_2} Data Obtained From 4 Separate Tumors and 7 Profiles*

Tumor no.	Viable P_{O_2} (mm Hg)	Necrotic P_{O_2} (mm Hg)
1	60–82	3–6
2	50–56	2–6
3	50–54	11–13
4	55–79	7–9

* P_{O_2} levels of 50–82 torr were associated with viable tissue, and 2–13 torr was associated with necrotic regions. P_{O_2} gradient from viable to necrotic regions ranged from 50–300 μ.

thus influencing electrode measurements recorded within the boundaries of this gradient.[10,11]

In contrast to previous experimentation, we 1) measured P_{O_2} profiles with a polarographic, recessed oxygen microcathode, which provided more accurate tissue P_{O_2}, and 2) used a controlled physiologic environment, which eliminated atmospheric P_{O_2} contamination in the tissue. First, regarding microcathode function, plots of current versus voltage for our microcathodes exhibited a standard plateau (usually -0.6 to -0.9 volts relative to the calomel reference half-cell). At this voltage, oxygen concentration has been known to be proportional to cathode current,[19] and we showed this for our microcathodes (Figure 2); at higher voltages hydrogen ion has been reduced at the cathode surface.[19] The electrochemical reduction of molecular oxygen at the gold cathode surface induced an oxygen diffusion field nearly completely within the recess.[7] We have evaluated microcathodes with varied lengths of tip recess through an unstirred oxygen equilibrated medium (2-mm gels of 3% agar in saline). Electrode current was observed to be a function of the ratio of recess length to lumen diameter; electrodes with ratios of 4:1 showed that approximately 95% of oxygen diffusional gradients were limited to the recess, and ratios of 10:1 showed approximately 99%. These values closely matched mathematical calculations,[7] and therefore the recessed microcathodes used for this experiment induced an insignificant P_{O_2} field that extended approximately 1–2 μ around the tip of the lumen. This was an important consideration, because oxygen concentration surrounding the electrode in tissue was variable. Other oxygen electrodes of the needle or bare-tipped type consumed larger amounts of oxygen and induced significant P_{O_2} diffusion fields into the surrounding electrode medium and have been inaccurate in tissue because electrode response "averaged" and indiscriminantly lowered the P_{O_2} of the surrounding tissue. Also, these electrodes (generally $\geqslant 10$ μ) were large, compared with cell size, and damaged or compressed tissue during penetration. Second, we corrected for error produced by diffusion of oxygen into the tumor surface by creating a well which was filled with oxygen-equilibrated BSS. During microcathode advancement into the tumor, the P_{O_2} in the well was approximately that of subcutaneous tissue, 25–30 torr. Previously, we demonstrated the importance of oxygen diffusion into exposed tissue by filling the well with a BSS of 90-torr P_{O_2} and then recorded P_{O_2} levels of tissue surface regions.[11] We observed that P_{O_2} gradients extended from the BSS into the tissue.

In addition to resolving questions with regard to the accuracy of tissue P_{O_2} levels, this experiment incorporated and combined techniques that permitted correlation of P_{O_2} levels in neoplasms with the structure of permanent tissue sections. To obtain tissue sections of the electrode measuring site that would maintain representative *in situ* dimensions we developed a freeze-exchange fixation process. The morphologic appearance of DMBA adenocarcinoma after freeze-exchange fixation is shown in Figures 4 and 5. Cellular detail was not apparent in these photomicrographs because the sections were cut at approximately 50 μ. In Figure 3, the overlying connective tissue of the hypodermis (H), for the most part, was intact. A remaining suture was visible in the upper left portion. The necrotic area (N) had become liquefied, while the periphery (P) of the neoplastic growth was vascular. Figure 4 showed vascular networks mantled by viable tumor cells, which were probably surrounded by severe hypoxia. Previous work in this laboratory has shown that the differences in structural dimensions of frozen sections examined at -30 C, compared with adjacent freeze-substituted sections, were statistically insignificant.[11] Cooled Freon 22 (approximately -160 C) was used for freezing the tissue and preceded nitrogen application because liquid nitrogen (-196 C) has a lower coefficient of heat transfer, and, also, an insulating vapor[16] can be formed just over the surface it cools. The quick freezing of tumor regions at the depth of microcathode puncture ($\leqslant 2$ mm) has been estimated[17] to occur in less than 2 seconds. Dr. Lloyd Back (personal communication, Section Leader, Fluid Mechanics of Heat and Mass Transfer Group, Jet Propulsion Laboratory, Pasadena, Calif) has calculated the freeze rate for an *in vivo* femoral arterial wall,[11] where arterial blood flow behaved as a heat sink, using the freezing methods described in this paper. Within 1 second, the depth of the freeze of the arterial wall would be greater than 0.5 mm; and by comparison, the tumor frozen in this study, which lacked the femoral artery heat sink effect, might have occurred more quickly.

This experimental protocol could routinely acquire tumor P_{O_2} profiles with frequent electrode calibration, and our belief has been that technical improvement and development might permit future acquisition of fundamental pathologic and therapeutic knowledge. Some pitfalls were apparent. First, animal stability during anesthesia was difficult to evaluate without knowledge of continuous blood pressure and blood gas values. These measurements should be incorporated into future experiments to examine ani-

mal stability. Second, a knowledge of arterial P_{O_2} could also suggest relationships between tissue P_{O_2} and regions of arterial blood supply, particularly since the structure of the walls of the vessels in these tumors was abnormal. Third, the ability to routinely cut thin, freeze-substituted sections (less than 8 μ) would provide microscopic cellular detail and could potentiate knowledge acquisition of oxygen tension over distances of one cell diameter. Finally, others have described techniques by which microelectrodes permanently mark the tissue during penetration.[20,21] Marking the electrode track on permanent freeze-substituted sections would enable even more exact intracellular P_{O_2} correlation with morphologic features.

In summary, we have concluded that the approach described here, with further technical development, could provide a foundation for the study of relationships between distribution of P_{O_2}, tumor cell death, neoplastic growth, and the oxygen environment of viable tumor cells. Such information has potential in the evaluation of the mechanisms of radiation therapy, hyperthermia, and oxygen inhalation in the inhibition of tumor growth.

References

1. Cater DB, Phillips AF, Silver IA: Apparatus and techniques for the measurement of oxidation-reduction potentials, Ph and oxygen tension in vivo. Proc Roy Soc B 1957, 146:289-297
2. Cater DB, Silver IA: Quantitative measurements of oxygen tension in normal tissues and in the tumours of patients before and after radiotherapy. Acta Radiol 1960, 53:233-256
3. Gullino PM, Grantham FH, Courtney AH: Utilization of oxygen by transplanted tumors in vivo. Cancer Res 1967, 27:1020-1030
4. Gunther H, Vaupel P, Metzger H, Thews G: Stationare Verteilung der O_4-brucke im Tumorgewebe DS-Carcinosarkom): I. Messungen in vivo unter Verwendung von Gold-Mikroelectroden. Z Kresforsch 1972, 77:26-39
5. Puffer HW, Warner NE, Schaeffer LD, Wetts RW, Bradbury M: Preliminary observations of oxygen levels in microcirculation of tumors in C3H mice, Oxygen Transport to Tissue. Vol 2. Edited by J Grote, D Reneau, G Thews. New York, Plenum Publishing Corp., 1976, pp 605-610
6. Vaupel P: Oxygen supply to malignant tumors, Tumor Blood Circulation: Angiogenesis, Vascular Morphology and Blood Flow of Experimental and Human Tumors. Edited by HI Peterson. Florida, CRC Press, 1979, pp 143-168
7. Schneiderman G, Goldstick TK: Oxygen electrode design criteria and performance characteristics recessed cathode. J Appl Physiol Respir Environ Exercise Physiol 1978, 45:145-154
8. Gray LH, Conger AD, Ebert M: The concentration of oxygen dissolved in tissues at the time of irradiation as a factor in radiotherapy. Br J Radiol 1953, 26:638-648
9. Del Monte U: Changes in oxygen tension of Yoshida ascites hepatoma during growth. Proc Soc Exp Biol Med 1967, 125:853-856
10. Vaupel P: Hypoxia in neoplastic tissue. Microvasc Res 1977, 13:399-408
11. Crawford DW, Back LH, Cole MA, Feldstein C, Paule WJ: In vivo oxygen transport in the normal rabbit femoral arterial wall. J Clin Invest 1980, 65:1498-1508
12. Whalen WJ, Riley J, Nair P: A microelectrode for measuring intracellular P_{O_2}. J Appl Physiol 1967, 23:798-801
13. Giese J: Acute hypertensive vascular disease. Acta Pathol Microbiol Scand 1964, 62:497-515
14. Whalen WJ, Nair P, Ganfield RA: Measurements of oxygen tension in tissues with a micro oxygen electrode. Microvasc Res 1973, 5:254-262
15. Kanabus EW, Feldstein C, Crawford DW: Excursion in vibrating microelectrodes in tissue. J Appl Physiol Respirat Environ Exercise Physiol 1980, 48:737-741
16. Staub NC, Storey WF: Relation between morphological and physiological events in lung studied by rapid freezing. J Appl Physiol 1962, 17:381-390
17. Sobin SS, Bernick S, Trember HM, Rosenquist TH, Lindal R, Fung YC: The fibroprotein network of the pulmonary interalveolar wall. Chest 1974, 65:45-55
18. Brown GB: An Introduction to Histotechnology. New York, Appleton-Century-Crofts, 1978
19. Davies PW: The oxygen cathode, Physical Techniques in Biological Research. Vol 4. New York, Academic Press, 1962, pp 137-179
20. West JR, Deadwyler SA, Cotman CW, Lynch G: A dual marking technique for microelectrode tracks and localization of recording sites. Electrocephal Clin Neurophysiol 1975, 39:407-410
21. Nair P, Spande JI, Whalen WJ: Marking the tip location of P_{O_2} microelectrodes or glass micropipettes. J Appl Physiol Respirat Environ Exercise Physiol 1980, 49:916-918